RSC Advances

PAPER

View Article Online
View Journal | View Issue

Cite this: *RSC Adv.*, 2017, **7**, 7140

Ethanol/acetaldehyde conversion into butadiene over sol–gel ZrO_2–SiO_2 catalysts doped with ZnO

Yuchao Xu,[ab] Zongzhang Liu,[ab] Zheng Han[ab] and Minhua Zhang*[ab]

Received 12th October 2016
Accepted 5th December 2016

DOI: 10.1039/c6ra25139k

www.rsc.org/advances

ZnO promoted ZrO_2–SiO_2 catalysts synthesized by a sol–gel method were investigated in the two-step ethanol transforming to 1,3-butadiene process. The influence of promoters and the preparation method of the catalysts on the catalytic performance were studied in detail and the reaction conditions were optimized. The as-prepared catalysts were characterized by BET, X-ray diffraction (XRD), Scanning Electron Microscopy (SEM), Transmission Electron Microscopy (TEM), Fourier Transform Infrared Resonance (FT-IR), X-ray photoelectron spectroscopy (XPS), FT-IR spectroscopy of adsorbed pyridine (Py-IR) and temperature-programmed desorption of NH_3 (NH_3-TPD). ZnO added ZrO_2–SiO_2 catalysts show the best catalytic activity and the catalysts prepared by the hybrid sol–gel method were superior to those prepared by the sol–gel coupled with impregnation method. The addition of promoters in the ZrO_2–SiO_2 system decreased the total acidity and lowered the selectivity to dehydration products. The best performance with ethanol/acetaldehyde conversion of 40.7% and 1,3-butadiene selectivity of 83.3% was reached at 310 °C, ethanol/acetaldehyde mole ratio of 3.5 and WHSV of 1.4 h^{-1} using a 0.5 wt% ZnO doped ZrO_2–SiO_2 catalyst.

1. Introduction

1,3-Butadiene (BD) is one of the most important bulk chemicals in the oil industry, and has been widely used in various fields of synthesis of rubber elastomers and resins. Generally, the ethanol to BD route is divided into two different parts, the one-step process and the two-step process. The former was first introduced by Lebedev, a USSR chemist, in the 1920s. The latter was a refined process by using an ethanol and acetaldehyde mixture as the feed, and was first commercialized by a US company, the Carbide and Carbon Chemicals Corporation.

In recent years, the supply and the price of BD largely depend on the supply of ethylene, one of bulk chemicals in oil industry. With the improvement on the technology of exploiting syngas in America and west Europe, there would be an shortage of the supply of BD in the near future.[1] Meanwhile, the technology of bio-ethanol has been improved dramatically and used widely all over the world. The bio-ethanol can be easily obtained not only from crops such as corn and sugarcane but also from inedible raw materials such as fibre and lignin.[2] In 2011, the output of ethanol worldwide was over 100 billion litres, which showed a fast growth. The production of high value-added products from bio-ethanol has been attracting interest from all over the world.

Ever since the commercialization of ethanol into BD, researchers have been studying the mechanism of this process for decades. Up to now, the mechanism is still in debate among studies, and a generally accepted reaction network was used in dozens of studies as reported in ref. 3–6. It's also believed that the mechanisms for one-step process and two-step process show no difference.[7] The generally accepted mechanism contains: (1) ethanol dehydrogenation into acetaldehyde; (2) aldol condensation of acetaldehyde into acetaldol; (3) dehydration of acetaldol into crotonaldehyde; (4) Meerwein–Ponndorf–Verley reaction of crotonaldehyde by ethanol; and (5) dehydration of crotyl alcohol into BD.

As reported in former literatures,[8,9] MgO–SiO_2 and ZrO_2–SiO_2 were regarded as the two most promising catalytic system in ethanol to BD process, each for one-step and two-step, respectively. Dozens of studies were performed on MgO–SiO_2 catalytic system.[5,10–13] While, only a few studies were conducted using ZrO_2–SiO_2 or ZrO_2–SiO_2 based catalysts in ethanol to BD process before 2010. Afterwards, systematic studies have been conducted by Vitaly L. Sushkevich *et al.* in order to choose the most active component, accommodate acid–base properties, and figure out the function of promoters. Many studies have been conducted on ZrO_2–SiO_2 or metal oxides promoted ZrO_2–SiO_2 system in the past five years, as reported in ref. 7, 14 and 15 Sushkevich *et al.*[7] revealed the excellent catalytic capacity of Ag promoted Zr-containing SiO_2 molecular sieve (Zr-MCM-41 and Zr-BEA) in the ethanol transforming to BD process. The best performance was obtained with the ethanol conversion of 48% and BD selectivity of 56% using 1 wt% Ag doped Zr-BEA catalyst.

[a]*Key Laboratory for Green Chemical Technology of Ministry of Education, R&D Center for Petrochemical Technology, Tianjin University, Tianjin 300072, P. R. China. E-mail: mhzhang@tju.edu.cn; Fax: +86-22-27401826; Tel: +86-22-27401826*

[b]*Collaborative Innovation Center of Chemical Science and Engineering, Tianjin, China*

Jian *et al.*[15] reported a Zr/MCF catalyst of high performance, which showed the highest 1,3-butadiene yield and selectivity at the WHSV of 3.7 h^{-1} and 1.5 h^{-1}, respectively. The former studies conducted by other researchers showed a possibility of industrial application of Zr–Si catalytic system in ethanol conversion to BD process.

In our previous work,[16] we reported the application of sol–gel ZrO_2–SiO_2 catalysts and gained a relatively high performance compared with the results in other references. Meanwhile, the selectivity to dehydration products remains high and the catalysts show a relatively poor durability on the long-time stability test. As reported,[5,10,17–19] the addition of promoters into MgO–SiO_2 system would be beneficial for elevating BD selectivity as well as prolonging catalyst life.

Thus, in this study, metal or metal oxide promoted ZrO_2–SiO_2 catalysts prepared *via* sol–gel method were characterized and their catalytic performances for the formation of BD from bioethanol and acetaldehyde were investigated. The effects of addition of promoters and preparation method of catalysts on the structure and acid properties were studied. The mass content of the best promoter was also optimized. The experimental conditions, *i.e.*, the reaction temperature, the mole ratio of ethanol to acetaldehyde and the WHSV were optimized. The long-time durability study was also conducted as to figure out the stability of the catalysts. Different characterization methods were used to explore the relevance of the type of promoters and acid properties to the catalytic performances.

2. Experimental

2.1 Chemicals and materials

Zirconium oxynitrate (AR), acetaldehyde (97%), magnesium nitrate hexahydrate (AR) were obtained from Aladdin Industrial Corporation, Shanghai, China. Tetraethyl orthosilicate (AR), zinc nitrate hexahydrate (AR), manganese nitrate (50% solution, AR), silver nitrate (AR) were purchased from Tianjin Guangfu Chemical Reagent Co., Ltd, Tianjin, China. Nitric acid (AR) was purchased from Beijing Chemical Works. Dry ethanol (AR) and pyridine were purchased from Tianjin Jiangtian Chemical Technology Co., LTD.

2.2 Catalyst preparation

All ZrO_2/SiO_2 catalysts were prepared by using sol–gel method as described in ref. 16. The ZrO_2 mass loading for all samples was 2%. Promoter ZnO was added by using two different methods: hybrid sol–gel method (HSG) and sol–gel, and impregnation method (SGI). The catalysts prepared by the former method were referred to as Zr–Si-A and the latter referred to as Zr–Si-B. In general, the HSG catalysts were synthesized through the same process as described in our previous work.[16] In particular, the precursor of the dopant, $Zn(NO_3)_2 \cdot 6(H_2O)$, with a mass content of 0.5%, and $ZrO(NO_3)_2$ were added simultaneously into the solvent before gelation process. The SGI catalysts were synthesized by incipient wetness impregnation of ZrO_2/SiO_2 catalysts with an aqueous solution of zinc nitrate hexahydrate to attain a ZnO mass content of 0.5%. After impregnation process, the catalyst was dried at 383 K for 6 h and calcined at 923 K for 6 h with a heating rate of 5 °C min^{-1}.

2.3 Catalyst characterization

N_2 adsorption–desorption isotherms (BET) were measured at −196 °C using a Micromeritics Tristar 3000 surface area and pore size analyser. Before measurement, all samples were pretreated at 300 °C for 6 h. The Brunauer–Emmett–Teller (BET) method was used here to calculate the surface areas.

Powder X-ray diffraction patterns (XRD) of the catalysts were taken using a Rigaku D/Max 2500 type X-ray powder diffractometer with Cu Kα radiation at a wavelength of 1.5456 Å with the scan range of 5–90° at the scan rate of 5° s^{-1}.

Scanning Electron Microscope (SEM) images were taken using a Hitachi S-4800 with the resolution of 1 nm. All the samples were ground thoroughly and treated with conductive coating before measurement, TEM images were obtained using a Tacnai G2 F20 electron microscope operating at 200 kV. All the samples were suspended in absolute ethanol with an ultrasonic dispersion for 0.5 h. The suspension was doped on a copper grid coated with amorphous carbon film before measurement.

The infrared spectra were obtained using a Nicolet 6700 spectrometer with the scanning range from 4000 to 400 cm^{-1} and at a resolution of 4 cm^{-1}. All the catalysts were prepared with the addition of KBr at the weight proportion of 99%.

X-ray photoelectron spectroscopy (XPS) spectra were taken on a PerkinElmer PHI-1600 spectrometer using an Mg Kα X-ray radiation source at the pressure of 3.0×10^{-7} Mbar. The collected binding-energy values were referenced to the C 1s line at 284.6 eV.

The acidic properties were studied using FT-IR spectroscopy of adsorbed pyridine. IR spectra were taken on a Nicolet 6700 FT-IR spectrometer with the optical resolution of 4 cm^{-1}. Before measurement, the samples were pretreated at 200 °C under a vacuum of 10^{-3} Pa for 2 h. Adsorption of pyridine was carried out at 110 °C, difference spectra were obtained by subtraction of the blank spectra of the catalyst samples at 110 °C from the spectra of the samples with adsorbate at correlated temperatures.

The quantity and strength of acidity were determined by NH_3-TPD method using a Micromeritic Autochem II 2920. All samples were pre-treated at 500 °C for two hours under a helium (99.999%) flow rate of 50 mL min^{-1}. After being cooled to 70 °C, the sample was saturated with ammonia (argon 99%, ammonia 1%) at a flow rate of 20 mL min^{-1} for 50 min and subsequently purged with He (30 mL min^{-1}) for 1 h to remove the physically adsorbed NH_3. Temperature programming process was then conducted at the range from 70 °C to 400 °C with a temperature ramp rate of 15 °C min^{-1} in helium at a flow rate of 50 mL min^{-1}. The signal of desorbed NH_3 was recorded by a Thermal Conductivity Detector (TCD).

2.4 Catalyst evaluation

The catalytic conversion of ethanol and acetaldehyde mixture into BD was performed on a fixed bed reactor. Before experiment, the samples were ground and sieved into 20–40 mesh. The mole ratio range of ethanol to acetaldehyde was 2.5–4.5.

The WHSV varied from 0.2 to 2.2 h^{-1}. The reaction temperature range was 290–340 °C. The dry gas was analysed online by Agilent 7890A gas chromatograph using a 30 m HP-PLOT-Q column. The products contain 1,3-butadiene (BD), ethylene (EL), propylene (PL), butylene (BL), ethyl acetate (EA), and diethyl ether (DE).

The conversion of ethanol and acetaldehyde mixture, and selectivity towards the products were calculated as follows:[20]

$$\text{Total conversion} = \frac{(\text{total } C \text{ moles} - (C_{\text{mole unreacted ET}} + C_{\text{mole unreacted AA}})\text{moles})}{\text{total } C \text{ moles}} \times 100$$

$$\text{Selectivity} = \frac{C \text{ mole}_{\text{products}}}{\text{total } C \text{ moles} - (C_{\text{mole unreacted ET}} + C_{\text{mole unreacted AA}})\text{moles}} \times 100$$

3. Results and discussion

3.1 Catalyst characterization

3.1.1 Catalyst structure and composition. The physical properties of as-prepared catalysts were listed in Table 1. The addition of promoters in Zr–Si decreased S_{BET}, average pore size and pore volume to some extent. This can be explained by blockage of SiO_2 pores when promoters were added through sol–gel process. The addition method of ZnO promoter had a great impact on the physical properties of ZnO promoted Zr–Si catalysts. As can be seen (line 6 and line 9), the S_{BET}, average pore size and pore volume in $Zn_{1.0}$–Zr–Si-A were much higher than those of $Zn_{1.0}$–Zr–Si-B, which proved to be an highly dispersed ZnO species in $Zn_{1.0}$–Zr–Si-A sample compared with an relatively larger ZnO particle size which in turn caused the blockage of pores in $Zn_{1.0}$–Zr–Si-B sample. Different ZnO loadings showed no obvious changes on the physical properties of the catalysts (line 7 to line 12). Only a slight decrease was observed on these parameters.

XRD was performed in order to study the difference of the structure of two methods, as shown in Fig. 1. No typical peaks of SiO_2 or ZrO_2 were found for three samples, only a halo at around $2\theta = 23.0°$ was obvious in all patterns, which can be explained as a well dispersed state of ZrO_2 on SiO_2 surface.[21,22] As to ZnO promoted Zr–Si catalysts, a typical halo was also shown at $2\theta = 23.0°$. At lower ZnO loadings, no typical peaks of ZnO were recorded, which means a well dispersed state of ZnO species on SiO_2 surface.[23,24] When ZnO loading increased up to 4.0 wt%, some typical peaks at $2\theta = 31.767°$, 34.421°, 36.252°, 56.592°, 62.856° and 67.945° were observed, which were assigned to (100), (002), (101), (110), (103), (112) crystal face of ZnO (JCPDS 36-1451), respectively.

Table 1 Pore structural characteristics of the catalysts

Line	Sample	S_{BET} (m^2 g^{-1})	d (Å)	V (cm^3 g^{-1})
1	Zr–Si	601	26.1	0.39
2	$Cu_{1.0}$–Zr–Si-A	544	24.3	0.33
3	$Ag_{1.0}$–Zr–Si-A	614	23.9	0.37
4	$Mn_{1.0}$–Zr–Si-A	448	24.1	0.27
5	$Mg_{1.0}$–Zr–Si-A	561	25.0	0.34
6	$Zn_{1.0}$–Zr–Si-B	514	23.1	0.30
7	$Zn_{0.25}$–Zr–Si-A	607	25.6	0.38
8	$Zn_{0.5}$–Zr–Si-A	594	25.5	0.36
9	$Zn_{1.0}$–Zr–Si-A	570	25.2	0.36
10	$Zn_{2.0}$–Zr–Si-A	580	25.4	0.37
11	$Zn_{4.0}$–Zr–Si-A	568	25.1	0.36
12	$Zn_{8.0}$–Zr–Si-A	548	24.5	0.36

SEM and TEM characterizations were conducted to confirm the information resulted from XRD patterns. Comparing the SEM images in Fig. 2a and b, it's obvious that the particles size in Fig. 2a was smaller and smoother than that in Fig. 2b, which indicated a well-dispersed state of ZrO_2 and ZnO on SiO_2 through hybrid sol–gel method. TEM images in Fig. 2c and d exhibited a better sight of the morphology of two types of catalysts. In Fig. 2c, no observable ZrO_2 or ZnO particles were found at the scale of 200 nm, which elucidated a well dispersed state of amorphous ZrO_2 and ZnO on silica support. While in Fig. 2d, the agglomeration of the particles can be seen at the same scale of Fig. 2c. But no crystal ZrO_2 or ZnO was found in the map, implying that ZrO_2 and ZnO were at amorphous state. The results obtained from SEM and TEM images were in good agreement with that of XRD patterns.

In order to verify the interaction between ZnO, ZrO_2 and SiO_2 phase, FT-IR studies of SiO_2, ZrO_2/SiO_2, $Zn_{1.0}$–Zr–Si, $Zn_{1.0}$–Zr–Si-B were performed. In Fig. 3, some typical wavenumbers were shown at 400–2200 cm^{-1}. In particular, wavenumbers at 1082 cm^{-1} and 1223 cm^{-1} were assigned to ν_{as}(Si–O–Si),[25,26] wavenumbers at 804 cm^{-1} and 463 cm^{-1} were assigned to ν_s(Si–O–Si)[26,27] and wavenumber at 1631 cm^{-1} was assigned to physisorbed water on silica phase.[28]

It has been noted in ref. 29 that typical adsorption of Si–OH at 960 cm^{-1} can be observable on silica surface at low calcination temperatures, while at high temperatures, it disappears. This can be explained as the dehydration of Si–OH groups forming Si–O–Si moieties. But in the present work, a different condition was observed, even the samples were calcinated at a relatively high temperature (650 °C), and a similar band at 964 cm^{-1} remained distinct for SiO_2 sample (line a in Fig. 3).

For SiO_2 supported metal oxides, the vibration peaks at 962–970 cm^{-1} band is assigned to the metals incorporated into the framework of the mesoporous silica materials.[30] When metals are incorporated into silica phase, the intensity of this band increases, which is generally considered as a proof of the incorporation of hetero-atoms into the silica framework. In the present study, the wavenumber, at around 964 cm^{-1}, can be described as the formation of Zr–O–Si structure with the transition of Zr atoms into silica framework.[21,31]

XPS was conducted in order to study the chemical states of ZnO and ZrO_2 on silica surface and the forms it combined between ZnO, ZrO_2 and SiO_2. In the present work, ZnO was added as the promoter. Meanwhile, as depicted in the XRD patterns, no characteristic peaks of ZnO were detected, which may indicate a strong interaction between ZnO and SiO_2.

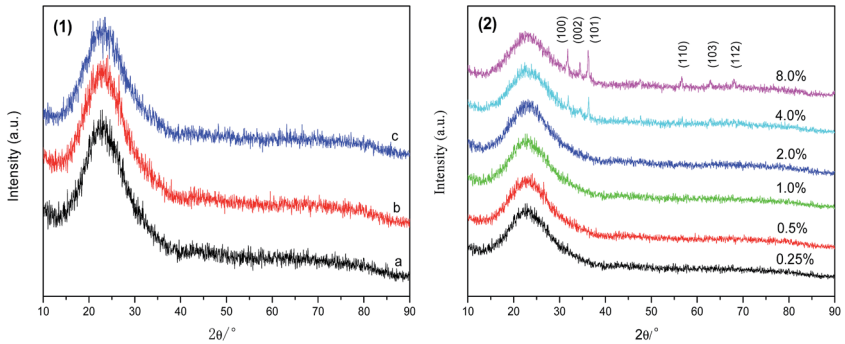

Fig. 1 XRD patterns for the catalysts (1) catalyst samples prepared by different method (a) Zr–Si; (b) $Zn_{1.0}$–Zr–Si-A; (c) $Zn_{1.0}$–Zr–Si-B; (2) catalyst samples with different ZnO contents.

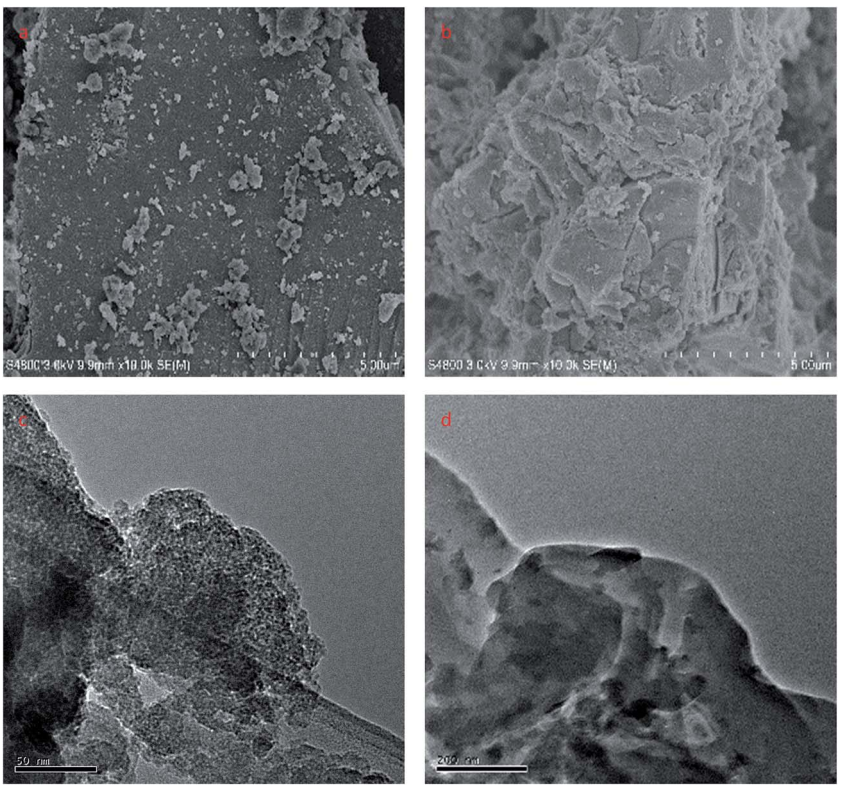

Fig. 2 SEM image (5 μm) of (a) $Zn_{1.0}$–Zr–Si-A, (b) $Zn_{1.0}$–Zr–Si-B. TEM image of (c) $Zn_{1.0}$–Zr–Si-A (50 nm), (d) $Zn_{1.0}$–Zr–Si-B (200 nm).

Considering this point of view, XPS profiles of Zn 2p were shown in Fig. 4A. As for $Zn_{1.0}$–Zr–Si-B, the binding energy of Zn 2p was 1022.7 eV, which means ZnO was more likely presented as bulk ZnO[32] (binding energy varies from 1021.8 eV to 1022.5 eV) on SiO_2 surface. On the contrary, the binding energy of Zn 2p for $Zn_{1.0}$–Zr–Si-A sample was significantly higher than that of bulk ZnO. The shift of the binding energy of Zn 2p was reported in ZnO–SiO_2 catalysts.[23,33] Upon ZnO loading, the binding energy of Zn 2p in ZnO–SiO_2 catalysts shifted to lower values compared with that of bulk ZnO, because the valence electron density of Zn in the Si–O–Zn bond is lower than that in the Zn–O–Zn bond.[23] Meanwhile, in the present study, this shift towards higher values was due to the strong interaction between ZnO and ZrO_2, which may be presented by Zn–O–Zr bonds, rather than the interaction between ZnO and SiO_2. The results indicated the existence of a Zn–Zr synergistic interaction in these catalysts.

Generally, synergistic effect of the promoter and loading components may affect binding energy in XPS results. As shown in Fig. 4B, the binding energy of Zr 3d for three samples was higher than that of bulk ZrO_2. According to Sushkevich, Vitaly L. *et al.*,[7] this phenomenon can be explained by the formation of Zr–O–Si bonds upon ZrO_2 loading through sol–gel process, which confirmed the result of FT-IR study. Interestingly, when comparing the result of curve (a) and curve (b) or curve (b) and curve (c), one may find that the binding energy of $Zn_{1.0}$–Zr–Si-B

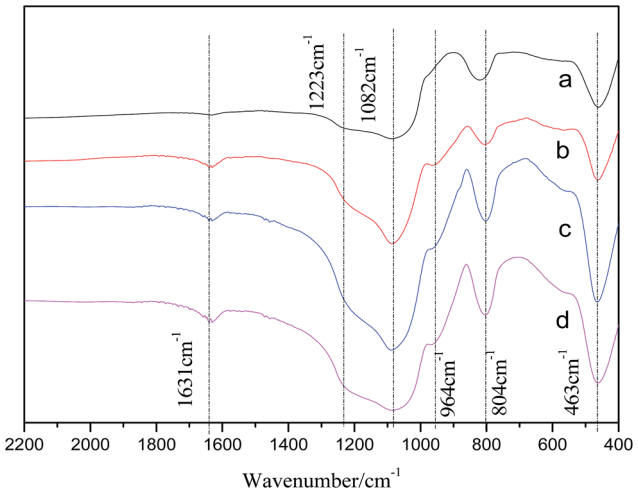

Fig. 3 IR spectra of the samples: (a) SiO_2; (b) Zr–Si; (c) $Zn_{1.0}$–Zr–Si-B; (d) $Zn_{1.0}$–Zr–Si-A.

was similar to that of the blank sample Zr–Si. Meanwhile, binding energy of $Zn_{1.0}$–Zr–Si-A was much higher than that of the counterparts, which also implied the interaction between ZnO and ZrO_2 in sol–gel process. As a result, binding energies of both ZnO and ZrO_2 were shifted to higher values.

3.1.2 Acidic properties of the catalysts. Quantity of acid for fresh samples was detected by thermal programmed desorption (TPD) using NH_3 as probe molecule. As shown in Fig. 5, NH_3 desorption signal was recorded at the range from 100 °C to 200 °C. Only a broad peak was found for all samples, this peak can be assigned to NH_3 adsorbed on weak acid sites.[34] The relative quantity of acidity was calculated as shown in Table 2. Interestingly, the blank catalyst Zr–Si showed the highest quantity of acidity. With different promoters loaded on Zr–Si catalyst, the quantity of acidity dropped to some extent, which may result from the coverage of Lewis acid sites formed on the inter-surface of ZrO_2 and SiO_2 by promoters through preparation process. Baylon *et al.*[35] also reported a similar phenomenon in Zn–Zr catalytic system used in ethanol conversion to BD process.

As for the strength of acidity, temperatures vary from 119 °C to 136 °C, $Mg_{1.0}$–Zr–Si-A shows the highest strength of acidity with a temperature of peak at 136 °C. No change of $Zn_{1.0}$–Zr–Si-A was found compared with blank catalyst Zr–Si in terms of temperature of peaks. The preparation method of catalyst often shows impact on the acid–base properties of the catalyst, *i.e.*, quantity and strength of acidity. A comparison of quantity and strength of acidity between $Zn_{1.0}$–Zr–Si-A and $Zn_{1.0}$–Zr–Si-B (line 9 and line 6, Table 2) was shown. No big difference was recorded on the quantity of acidity, while the temperature of NH_3 desorption peaks for $Zn_{1.0}$–Zr–Si-B sample was higher than that for $Zn_{1.0}$–Zr–Si-A sample.

Upon increasing ZnO loadings, quantity of acidity decreased lineally from 0.12 mmol g^{-1} to 0.03 mmol g^{-1} (line 7–12), which means the majority of acidity was suppressed by ZnO. While as to the strength of acidity, no big changes were found in different ZnO loading samples. However, as we can see, the temperature of NH_3 desorption peaks were shifted to higher values, implying a relatively higher strength of acidity resulted from large amount of ZnO (bulk crystal) in the ZrO_2–SiO_2 system, as revealed in XRD patterns and TEM images.

In conclude, the importance of acid properties has been revealed in former literatures,[17,18] but few systematic study has been conducted as to the relevance and weight between the quantity and strength of acidity in ZrO_2–SiO_2 catalytic system. Combining the results of the NH_3-TPD with catalytic performances of catalysts in this work, we predicted boldly that the strength of acidity was more important than quantity of acidity as to improving catalytic performance. A moderate strength of acidity should be essential for high catalytic performance of the catalyst.

In this work, an ordered study was performed by Py-IR to analyze the acid type of acid site of as-prepared catalysts. As reported,[35] the adsorption at 1450 cm^{-1} and 1608 cm^{-1} were typical bands of pyridine adsorbed on Lewis acid sites, 1490 cm^{-1} was assigned to pyridine adsorbed on both Lewis and Bronsted acid sites. For all promoter added catalysts, two bands at *ca.* 1590 cm^{-1} and 1445 cm^{-1} were observed, which showed a little gap from the typical bands of Lewis acid sites. Flanigen *et al.*[36] described this shifts to lower wavenumbers as the change

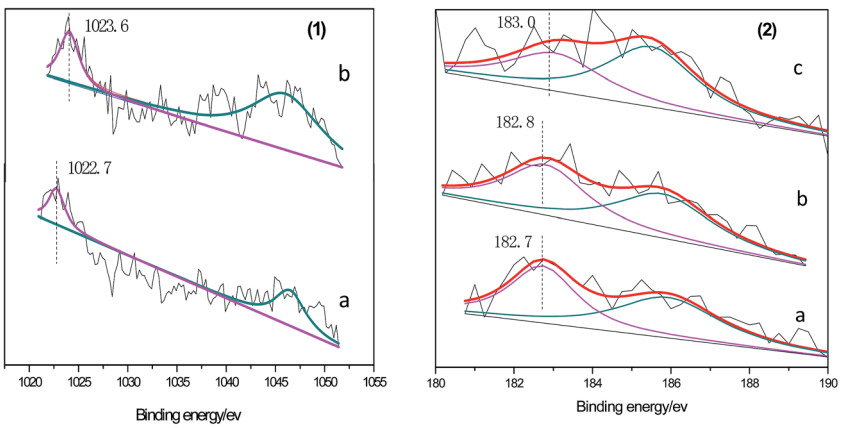

Fig. 4 (1) XPS profiles of Zn 2p (a) $Zn_{1.0}$–Zr–Si-B; (b) $Zn_{1.0}$–Zr–Si-A; (2) XPS profiles of Zr 3d for: (a) Zr–Si; (b) $Zn_{1.0}$–Zr–Si-B; (c) $Zn_{1.0}$–Zr–Si-A.

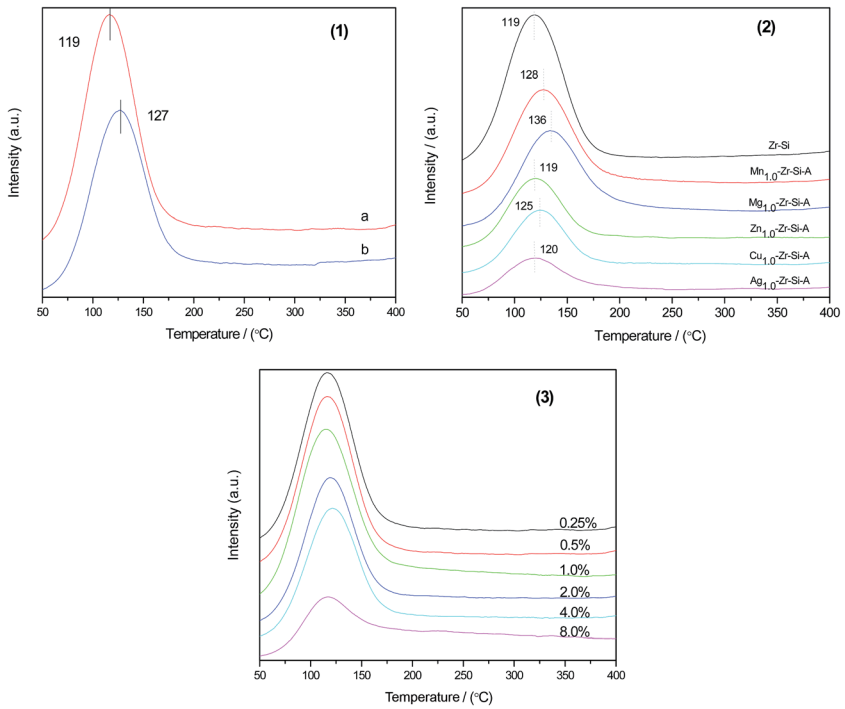

Fig. 5 NH_3-TPD profiles of (1) Zn–Zr–Si catalysts prepared by two different methods: (a) $Zn_{1.0}$–Zr–Si-A; (b) $Zn_{1.0}$–Zr–Si-B; (2) different mental oxide promoted Zr–Si catalysts; (3) Zn–Zr–Si-A catalyst samples with different ZnO contents.

Table 2 The acid properties of the catalysts

Line	Sample	Quantity of acidity (mmol g^{-1})	Temperature of NH_3 desorption peaks (°C)
1	Zr–Si	0.18	119
2	$Mn_{1.0}$–Zr–Si-A	0.13	128
3	$Mg_{1.0}$–Zr–Si-A	0.12	136
4	$Cu_{1.0}$–Zr–Si-A	0.07	125
5	$Ag_{1.0}$–Zr–Si-A	0.05	120
6	$Zn_{1.0}$–Zr–Si-B	0.08	127
7	$Zn_{0.25}$–Zr–Si-A	0.12	119
8	$Zn_{0.5}$–Zr–Si-A	0.08	119
9	$Zn_{1.0}$–Zr–Si-A	0.09	119
10	$Zn_{2.0}$–Zr–Si-A	0.07	121
11	$Zn_{4.0}$–Zr–Si-A	0.06	124
12	$Zn_{8.0}$–Zr–Si-A	0.03	120

of the diameter or positive charge of cations forming acid sites. As can be seen in Fig. 6a, acid types for different promoter added samples were mostly presented as Lewis acid sites. No distinct Bronsted acid, which shown typical adsorption peak at around 1540 cm^{-1}, was observable in the spectra of Zr–Si, $Zn_{1.0}$–Zr–Si-A, $Cu_{1.0}$–Zr–Si-A and $Ag_{1.0}$–Zr–Si-A samples. Meanwhile, the band at 1490 cm^{-1}, was distinguishable in the spectra of Mn and Mg promoted samples. For ZnO promoted samples, as shown in Fig. 6b, the bands at *ca.* 1445 cm^{-1} and 1590 cm^{-1} were evident. No obvious bands of Bronsted acid sites were recorded at low ZnO loadings. Meanwhile, some observable bands at *ca.* 1490 cm^{-1}, 1565 cm^{-1} and 1580 cm^{-1} were found when ZnO loading was higher than 4 wt%, which means new acid sites were formed on bulk crystal ZnO surface,[37,38] as analysed by XRD patterns. Interestingly, upon increasing ZnO loadings the band of Lewis acid sites at *ca.* 1590 cm^{-1} was shifted toward higher wavenumbers. This was in agreement with the study performed by Baylon *et al.*[35] They have explained this phenomenon as an increase of Lewis acid strength, which was in good agreement NH_3-TPD results in the present work.

3.2 Catalyst evaluation in ethanol conversion into butadiene

3.2.1 Catalytic activity. Catalytic evaluation study was performed under the condition of 320 °C with an ethanol/acetaldehyde mole ratio of 3.5, WHSV of 1.8 h^{-1}. As shown in Table 3, the main product and by-product distribution remained unchanged. Ethylene, butadiene, propylene, butylene, diethyl ether, and butanol were detected, which were simplified as EL, BD, PL, BL, DE, BU, and EA, respectively.

As shown in Table 3, among the testing results for different metal oxide promoted catalysts (line 2–6), the highest BD selectivity, 83.0%, was achieved using $Zn_{1.0}$–Zr–Si-A catalyst. Moreover, the conversion of $Zn_{1.0}$–Zr–Si-A was also the best. The addition of ZnO can boost the dehydrogenation ability in ethanol conversion to acetaldehyde process as well as MPV reaction of crotonaldehyde. Combining the analysis results above, the addition of ZnO into Zr–Si catalytic system did decrease the quantity of acidity to some extent, though, no changes were observed as to the acid strength and acid type. It can be inferred that moderate acid type and strength was critical to the process of ethanol conversion to BD. The addition of

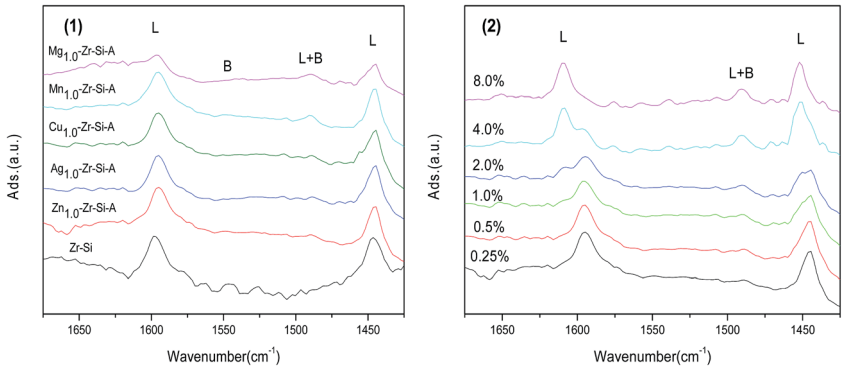

Fig. 6 (1) Py-IR spectra of Py-IR spectra of different promoters doped ZrO_2/SiO_2 catalysts and (2) Zn–Zr–Si-A catalyst samples with different ZnO contents.

Mn and Mg into ZrO_2–SiO_2 system didn't inhibit the formation of dehydration products such as EL and DE effectively (line 4 and 5). Combining the result of NH_3-TPD and Py-IR with the catalytic performance of due catalysts, one can predict that the increase of the quantity of acidity and the formation of Bronsted acid sites for Mn and Mg added samples may cause the decrease on the activity. Generally, Cu and Ag were regarded as dehydrogenation promoters, as reported in ref. 17, 19 and 39 which in turn, boosted BD selectivity. However, in this study, Cu and Ag showed inferior catalytic performances to that of other promoters, the BD selectivity was even lower than that of blank ZrO_2–SiO_2. The addition of Cu introduces redox-active sites which can boost dehydrogenation process of ethanol into acetaldehyde and inhibit the dehydration of ethanol. By the meantime, CuO can also poison acid site of the catalyst, which lowers the ethanol/acetaldehyde conversion and the selectivity to dehydration products (as shown in line 2).[19] The dehydrogenation ability of Ag was inferior to that of CuO, and more dehydration products (EL and DE) were formed at the expense of lower BD selectivity. Therefore, as analysed above, ZnO was chosen as the best promoter in this study.

As known to all, the method of promoter addition also had a great impact on the conversion of ethanol and acetaldehyde and BD selectivity. Obviously, the conversion of ZnO added ZrO_2–SiO_2 fresh sample through SGI process (line 7) dropped dramatically compared with ZrO_2–SiO_2 counterpart (line 1). This can be explained by the formation of bulk crystal of ZnO in SGI samples, which caused the blockage of pores, as analysed by BET, XRD, TEM and XPS. Whereas highly dispersed ZnO species obtained by HSG method on ZrO_2–SiO_2 surface can effectively decrease the quantity of acidity of Zr–Si without much difference on the strength of acid sites, which hindered the dehydration property of Zr–Si catalyst and boosted BD selectivity by the meantime (line 6).

It's also eye-catching that upon different promoters loading on Zr–Si system, the conversion of promoted samples dropped to some extent compared with that of Zr–Si counterpart. This can be explained as the decrease of acidity of those promoted samples. A relatively low acidity of the catalyst means some amount of active sites of Zr–Si system was reduced or covered by those metal oxides.

The catalytic data with different ZnO loading was shown in Table 3 (line 2, 3–8). When ZnO loading increased from 0.25

Table 3 Activity evaluation results of the catalysts at 320 °C, WHSV of 1.8 h^{-1} and ethanol/acetaldehyde mole ratio of 3.5 for 10 h

			Selectivity (*C*, mol%)							
Line	Sample	Con (%)	EL	PL	BL	BD	DE	EA	BU	C6+[a]
1	Zr–Si	42.2	13.5	1.5	0.8	66.0	12.6	1.6	0.8	3.0
2	$Cu_{1.0}$–Zr–Si-A	22.3	3.8	0	20.3	38.8	7.4	6.5	3.6	19.6
3	$Ag_{1.0}$–Zr–Si-A	15.9	10.2	0.9	0.6	70.0	10.9	1.6	0	5.8
4	$Mn_{1.0}$–Zr–Si-A	27.9	5.9	0.3	0.5	76.8	9.0	1.1	0.3	6.2
5	$Mg_{1.0}$–Zr–Si-A	27.0	11.1	1.5	0.7	75.3	8.1	0.8	0	2.6
6	$Zn_{1.0}$–Zr–Si-A	33.2	6.3	1.5	0.7	83.0	3.6	1.4	0.6	3.1
7	$Zn_{1.0}$–Zr–Si-B	19.1	4.8	0.7	0.7	72.2	13.3	1.8	1.1	5.5
8	$Zn_{0.25}$–Zr–Si-A	34.3	5.5	1.8	0.4	82.1	2.0	1.3	1.5	5.6
9	$Zn_{0.5}$–Zr–Si-A	36.8	5.1	1.4	0.4	83.5	3.7	1.1	0.2	4.8
10	$Zn_{2.0}$–Zr–Si-A	30.4	5.7	1.2	0.6	80.9	5.0	1.9	0.8	4.3
11	$Zn_{4.0}$–Zr–Si-A	35.0	9.8	1.3	0.6	78.1	5.9	1.4	0.3	2.7
12	$Zn_{8.0}$–Zr–Si-A	36.1	11.6	1.0	0.5	74.7	6.9	1.6	0.4	3.5

[a] Unidentified heavier compounds in GC chromatography.

wt% to 8.0 wt%, no big change on the ethanol and acetaldehyde mixed conversion was observed, with a conversion range from 30% to 37%. Meanwhile, selectivity to dehydration products (EL and DE) increased at the expense of lower BD selectivity. Notably, the maximum of BD selectivity, 83.5%, was reached at the ZnO loading of 0.5 wt%.

3.2.2 Effect of reaction temperature. Different parameters, *i.e.*, reaction temperature, ethanol/acetaldehyde mole ratio and WHSV were studied as to optimize the reaction conditions and $Zn_{0.5}$–Zr–Si-A was chosen as a representative sample. The results were shown in Fig. 7. As shown in Fig. 7a, with increasing temperature from 290 to 400 °C, the ethanol/acetaldehyde conversion increased gradually. Whereas BD selectivity increased at the range of 290 to 310 °C and then dropped hereafter. The maximum of BD selectivity, 84.2%, was reached at 310 °C, WHSV of 1.8 h^{-1}, ethanol/acetaldehyde mole ratio of 3.5. Moreover, the selectivity to EL and DE increased upon increasing reaction temperature. This reflected that high temperatures favour ethanol dehydration process.[40,41] Notably, at higher temperatures, the selectivity to heavier compounds C6+ tend to decrease. Given all the analysis above, 310 °C was chosen as the optimum reaction temperature in ethanol and acetaldehyde conversion to BD process.

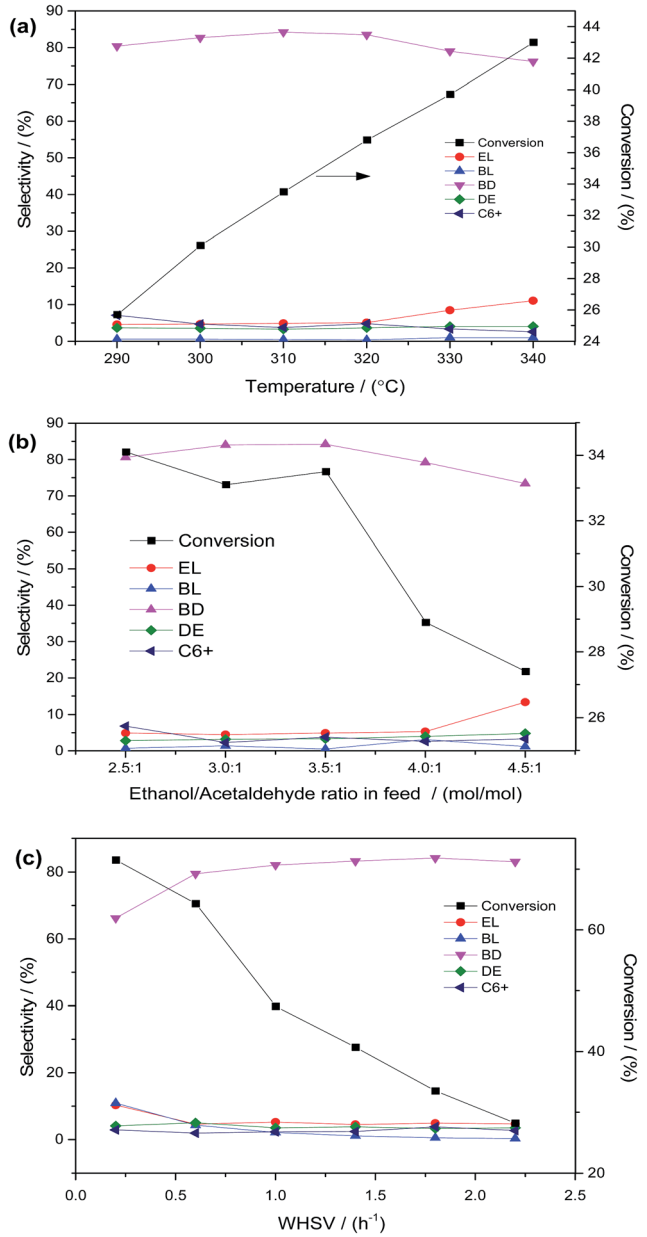

Fig. 7 Effect of (a) temperature; (b) ethanol/acetaldehyde mole ratio and (c) WHSV on the ethanol/acetaldehyde conversion and BD selectivity.

3.2.3 Effect of ethanol/acetaldehyde mole ratio. The optimum study on the ethanol/acetaldehyde ratio was conducted based on the optimum reaction temperature as analysed previously with a WHSV of 1.8 h^{-1}. The range of ethanol/acetaldehyde mole ratio was from 2.5 to 4.5 and the results were shown in Fig. 7b. It is obvious that the ethanol/acetaldehyde conversion dropped with increasing ethanol/acetaldehyde mole ratios. At high ethanol/acetaldehyde values, the selectivity to dehydration products (EL and DE) were much higher than that of low ethanol/acetaldehyde values. It's generally accepted that ethanol dehydration process can proceed on both Lewis acid sites than Bronsted acid sites.[42] Lower amount of acetaldehyde in feed did not inhibit ethanol dehydration ability on Zr–Si based catalysts. The best BD selectivity was obtained at the ethanol/acetaldehyde mole ratio of 3.5.

3.2.4 Effect of WHSV. The effect of WHSV was also studied under the condition of 310 °C and ethanol/acetaldehyde mole ratio of 3.5. As can be seen from Fig. 7c, the ethanol/acetaldehyde conversion boosted lineally with decreasing WHSV values. The BD selectivity showed a maximum at the WHSV of 1.8 h^{-1}. Strangely, the decrease of WHSV in the present work didn't elevate BD selectively which was in contrast with the results in ref. 15 and 43. Notably, the selectivity to EL and BL shown a fast growing trend at lower WHSV values, this could be explained by longer contact time at lower WHSV values, which increased the dehydration possibility on the catalyst.

3.2.5 Durability test of catalyst. Considering the relatively inferior catalytic durability of the catalysts in ethanol and acetaldehyde conversion into BD process as reported previously in ref. 3, 10 and 17, a catalytic durability testing of $Zn_{0.5}$–Zr–Si-A sample was performed at 310 °C with ethanol/acetaldehyde mole ratio of 3.5, and WHSV of 1.8 h^{-1}. The catalytic result was shown in Fig. 8. As clearly revealed, during the first 20 h, the catalytic index, *i.e.*, the BD selectivity and the ethanol/acetaldehyde conversion, were relatively high and stable. After 20 h testing, a slight decrease on both BD selectivity and ethanol/acetaldehyde conversion was observed. This means some amount of coke was doped on the active sites of the catalyst, which in turn lowered the catalytic performance. After 45 h testing, both BD selectivity and ethanol/acetaldehyde fluctuated to some extent. Finally, after 60 h, as we can see, the catalytic performance dropped obviously with both BD selectivity and ethanol/acetaldehyde conversion 10% lower than that of the fresh sample. The durability testing in this work showed a super performance in terms of BD selectivity and

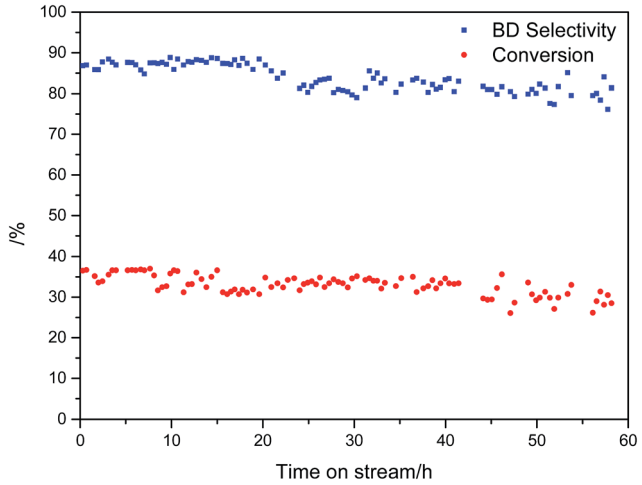

Fig. 8 The durability test of the catalysts.

ethanol/acetaldehyde conversion as well as high stability of the ZnO promoted Zr–Si catalyst. This result was in good agreement with the study conducted by Sekiguchi, Yasumasa *et al.*[10,43] They have pointed that a small amount of ZnO can prolong catalyst life dramatically. As is known, ZrO_2 was an high efficient component to catalysing condensation of acetaldehyde process[44] and much heavier compounds, referred to as C6+ in the present work, would be formed if adequate acetaldehyde was added into the feed. Those heavier compounds can be dehydrated or dehydrogenated on the surface of the catalyst and transformed into carbon species which may easily cover the active sites for catalysing ethanol to BD process. The addition of ZnO into ZrO_2–SiO_2 system may moderate the speed of acetaldehyde condensation process which in turn elevated the selectivity to BD and lowered the selectivity to C6+.

4. Conclusions

A series of metal oxide doped ZrO_2–SiO_2 catalysts were prepared by sol–gel method and used in the conversion of ethanol and acetaldehyde into 1,3-butadiene process. The catalysts prepared by hybrid sol–gel method showed better catalytic performances compared with those prepared by sol–gel coupled with impregnation method. ZnO was chosen as the best promoter for ZrO_2–SiO_2 catalytic system and $Zn_{0.5}$–Zr–Si-A catalyst showed the highest performance with 36.8% ethanol/acetaldehyde conversion and 83.5% BD selectivity. The reaction conditions were also optimized with 320 °C, 3.5 and 1.8 h^{-1} as the optimum reaction temperature, ethanol/acetaldehyde and WHSV, respectively. Acid studies showed the addition of ZnO into ZrO_2–SiO_2 system can decrease quantity of acidity yet didn't change the strength of acidity of the catalysts, which in turn lowered the selectivity to dehydration products and boosted BD selectivity simultaneously.

Acknowledgements

The authors thank the Key Laboratory for Green Chemical Technology of Ministry of Education of Tianjin University for technical support and the large precision instrument platform for XRD, XPS, SEM and HR-TEM measurements.

Notes and references

1 G. O. Ezinkwo, T. V. Philippovich, A. Auwal and I. A. Mamadshoevich, *ChemBioEng Rev.*, 2014, **1**, 194–203.
2 C. A. Cardona and Ó. J. Sánchez, *Bioresour. Technol.*, 2007, **98**, 2415–2457.
3 T. De Baerdemaeker, M. Feyen, U. Müller, B. Yilmaz, F.-S. Xiao, W. Zhang, T. Yokoi, X. Bao, H. Gies and D. E. De Vos, *ACS Catal.*, 2015, **5**, 3393–3397.
4 S. Bhattacharyya and S. Sanyal, *J. Catal.*, 1967, **7**, 152–158.
5 M. Lewandowski, G. S. Babu, M. Vezzoli, M. D. Jones, R. E. Owen, D. Mattia, P. Plucinski, E. Mikolajska, A. Ochenduszko and D. C. Apperley, *Catal. Commun.*, 2014, **49**, 25–28.
6 Y. Wang and S. Liu, *J. Bioprocess Eng. Biorefinery*, 2012, **1**, 33–43.
7 V. L. Sushkevich, I. I. Ivanova and E. Taarning, *Green Chem.*, 2015, **17**, 2552–2559.
8 B. Corson, H. Jones, C. Welling, J. Hinckley and E. Stahly, *Ind. Eng. Chem.*, 1950, **42**, 359–373.
9 S. Bhattacharyya and N. Ganguly, *J. Appl. Chem.*, 1962, **12**, 105–110.
10 Y. Sekiguchi, S. Akiyama, W. Urakawa, T.-r. Koyama, A. Miyaji, K. Motokura and T. Baba, *Catal. Commun.*, 2015, **68**, 20–24.
11 S. Kvisle, A. Aguero and R. P. A. Sneeden, *Appl. Catal.*, 1988, **43**, 117–131.
12 H. Niiyama, S. Morii and E. Echigoya, *Bull. Chem. Soc. Jpn.*, 1972, **45**, 655–659.
13 R. Ohnishi, T. Akimoto and K. Tanabe, *J. Chem. Soc., Chem. Commun.*, 1985, **22**, 1613–1614.
14 X. G. Jun-Kun Lai, A. Chakrabarti, J. Baltrusaitis and I. E. Wachs, *Catalytic Activity Testing from Ethanol to 1,3-butadiene on ZnO/ZrO_2/SiO_2*, Salt Lake City, UT, 2015.
15 L. C. Jian, Y. Shao, S. J. R. Tan, X. Li, Y. Zhang and S. L. Su, *ACS Sustainable Chem. Eng.*, 2016, **4**, 4887–4894.
16 Z. Han, X. Li, M. Zhang, Z. Liu and M. Gao, *RSC Adv.*, 2015, **5**, 103982–103988.
17 W. Janssens, E. V. Makshina, P. Vanelderen, F. De Clippel, K. Houthoofd, S. Kerkhofs, J. A. Martens, P. A. Jacobs and B. F. Sels, *ChemSusChem*, 2015, **8**, 994–1008.
18 O. V. Larina, P. I. Kyriienko and S. O. Soloviev, *Catal Lett.*, 2015, **145**, 1162–1168.
19 C. Angelici, M. E. Z. Velthoen, B. M. Weckhuysen and P. C. A. Bruijnincx, *ChemSusChem*, 2014, **7**, 2505–2515.
20 H.-J. Chae, T.-W. Kim, Y.-K. Moon, H.-K. Kim, K.-E. Jeong, C.-U. Kim and S.-Y. Jeong, *Appl. Catal., B*, 2014, **150**, 596–604.
21 Y. Zhang, L. Pan, C. Gao and Y. Zhao, *J. Sol-Gel Sci. Technol.*, 2011, **58**, 572–579.
22 R. G. R. Avendaño, J. A. D. L. Reyes, J. A. Montoya and T. Viveros, *J. Sol-Gel Sci. Technol.*, 2005, **33**, 133–138.
23 Q. Jiang, Z. Y. Wu, Y. M. Wang, Y. Cao, C. F. Zhou and J. H. Zhu, *J. Mater. Chem.*, 2006, **16**, 1536–1542.

24 Q. Yuan, N. Li, J. Tu, X. Li, R. Wang, T. Zhang and C. Shao, *Sens. Actuators, B*, 2010, **149**, 413–419.
25 S. K. Saha and P. Pramanik, *J. Non-Cryst. Solids*, 1993, **159**, 31–37.
26 T. Lopez, J. Navarrete, R. Gomez, O. Novaro, F. Figueras and H. Armendariz, *Appl. Catal., A*, 1995, **125**, 217–232.
27 D. M. Francisco, L. Willa and J. D. Mackenzie, *J. Am. Ceram. Soc.*, 2000, **83**, 1506–1512.
28 J. S. Loring, C. J. Thompson, Z. Wang, A. G. Joly, D. S. Sklarew, H. T. Schaef, E. S. Ilton, K. M. Rosso and A. R. Felmy, *Environ. Sci. Technol.*, 2011, **45**, 6204–6210.
29 H. S. Chen, Z. Y. Sun and J. C. Shao, *Bull. Chin. Ceram. Soc.*, 2011, **30**, 934–937.
30 K. M. Parida and S. S. Dash, *J. Mol. Catal. A: Chem.*, 2009, **306**, 54–61.
31 B. Hua, G. Qian, M. Wang and K. Hirao, *J. Sol-Gel Sci. Technol.*, 2005, **33**, 169–173.
32 M. Chen, X. Wang, Y. H. Yu, Z. L. Pei, X. D. Bai, C. Sun, R. F. Huang and L. S. Wen, *Appl. Surf. Sci.*, 2000, **158**, 134–140.
33 Z. Fu, B. Yang, L. Li, W. Dong, C. Jia and W. Wu, *J. Phys.: Condens. Matter*, 2003, **15**, 2867–2873.
34 J. Gao, J. Guo, D. Liang, Z. Hou, J. Fei and X. Zheng, *Int. J. Hydrogen Energy*, 2008, **33**, 5493–5500.
35 R. A. Baylon, J. Sun and Y. Wang, *Catal. Today*, 2016, **259**, 446–452.
36 E. M. Flanigen, in *Zeolite Chemistry and Catalysis*, ed. J. A. Rabo, ACS Monograph 171, American Chemical Society, Washington, DC, 1976, vol. 80.
37 A. Zecchina, C. Lamberti and S. Bordiga, *Catal. Today*, 1998, **41**, 169–177.
38 T. H. Mahato, G. K. Prasad, B. Singh, J. Acharya, A. R. Srivastava and R. Vijayaraghavan, *J. Hazard. Mater.*, 2009, **165**, 928–932.
39 C. Angelici, B. M. Weckhuysen and P. C. A. Bruijnincx, *ChemSusChem*, 2013, **6**, 1595–1614.
40 S. Freni, N. Mondello, S. Cavallaro, G. Cacciola, V. N. Parmon and V. A. Sobyanin, *React. Kinet. Catal. Lett.*, 2000, **71**, 143–152.
41 Y. Chen, Y. Wu, L. Tao, B. Dai, M. Yang, Z. Chen and X. Zhu, *J. Ind. Eng. Chem.*, 2010, **16**, 717–722.
42 S. H. Chai, H. P. Wang, Y. Liang and B. Q. Xu, *Green Chem.*, 2007, **9**, 1130–1136.
43 M. D. Jones, C. G. Keir, C. D. Iulio, R. A. M. Robertson, C. V. Williams and D. C. Apperley, *Catal. Sci. Technol.*, 2011, **1**, 267–272.
44 V. Ordomsky, V. Sushkevich and I. Ivanova, *J. Mol. Catal. A: Chem.*, 2010, **333**, 85–93.